The ITER core imaging x-ray spectrometer: X-ray calorimeter performance[a)]

P. Beiersdorfer,[1] G. V. Brown,[1] J. Clementson,[1] J. Dunn,[1] K. Morris,[1] E. Wang,[1] R. L. Kelley,[2] C. A. Kilbourne,[2] F. S. Porter,[2] M. Bitter,[3] R. Feder,[3] K. W. Hill,[3] D. Johnson,[3] and R. Barnsley[4]
[1]*Lawrence Livermore National Laboratory, Livermore, California 94550, USA*
[2]*NASA Goddard Space Flight Center, Greenbelt, Maryland 20771, USA*
[3]*Princeton Plasma Physics Laboratory, Princeton, New Jersey 08543, USA*
[4]*ITER Cadarache JWS, Cadarache Centre, 13108 St Paul-Les-Durance, France*

(Presented 19 May 2010; received 16 May 2010; accepted 7 September 2010; published online 26 October 2010)

We describe the anticipated performance of an x-ray microcalorimeter instrument on ITER. As part of the core imaging x-ray spectrometer, the instrument will augment the imaging crystal spectrometers by providing a survey of the concentration of heavy ion plasma impurities in the core and possibly ion temperature values from the emission lines of different elemental ions located at various radial positions. © *2010 American Institute of Physics.* [doi:10.1063/1.3495789]

I. INTRODUCTION

The core ion temperature and core bulk ion velocity of plasmas in the ITER tokamak (which is Latin for "the way") will likely be derived from the Doppler broadening and shift of x-ray lines emitted by highly charged tungsten ions.[1] The lines will be recorded by the core imaging x-ray spectrometer (CIXS), which will produce time-dependent radial profiles using the imaging views provided by four high-resolution crystal spectrometers. The instrument will be trained on a very narrow spectral range, which contains the strong $3d \rightarrow 2p$ resonant transition of neonlike W^{64+} and a few lines from neighboring charge states of tungsten. There is also the possibility of measuring the emission lines of heliumlike iron in discharges or time periods of a given discharge in which the electron temperature is rather low (<10 keV).

There is an inherent risk with monitoring only the lines of a few charge states or just one impurity at a given time. For example, if the particular ion is narrowly confined in the center, it may be impossible to obtain a radial profile. Similarly, iron or tungsten may not be sufficiently abundant in the core to obtain a signal, and the instrument may be thought to malfunction. In order to mitigate risks, it was suggested that the CIXS also include an x-ray microcalorimeter spectrometer.[1] Here we discuss some of the conceptual details of the microcalorimeter portion of the CIXS.

We note that the x-ray microcalorimeter instrument can simultaneously cover the entire soft x-ray spectral band. Such an instrument will thus provide the concentration of essentially all high-Z impurities and thus Z_{eff}. It will provide a measurement of the bremsstrahlung background and thus give a measure of the sightline integrated electron temperature. The instrument might also be capable of giving a crude radial profile of the ion temperature, and it might do so with moderate time resolution.

II. CIXS OVERVIEW

The conceptual design of the CIXS located in equatorial port number 9 is shown in Fig. 1. The imaging "fan" corresponding to each of the four crystal spectrometers is indicated, whereby two fans provide radial coverage of the upper half of the ITER plasma and two fans provide toroidal coverage. Also indicated, but barely noticeable because of its footprint, is the sightline of the microcalorimeter.

The CIXS shares the space in the port plug with several other diagnostics, i.e., the visible-infrared camera, the electron cyclotron system, and the toroidal interferometer/polarimeter. Some of the components of these systems are also indicated in Fig. 1.

The microcalorimeter requires only a <1 in. diameter radial sightline through the core of the plasma. Because the x-ray emission rate of ITER is extremely high over a broad photon range, the actual detector can be located 10s of meters away from the plasma and still be exposed to an x-ray flux that would exceed its intrinsic count rate ability, if most of the lower-energy flux were not attenuated by appropriately chosen attenuation foils. The exact details have not yet been fixed; however, conceptually, these attenuation foils will be chosen to "flatten" what is otherwise an exponentially varying x-ray flux from bremsstrahlung.

A microcalorimeter is similar to a bolometer except that it measures transient rather than continuous power.[2] In a microcalorimeter, the energy of a given x ray impinging on the detector is measured by recording the associated rise in temperature of the device. This means the detector is sensitive to neutrons, as the temperature rises each time a neutron deposits energy in the microcalorimeter. In order to prevent undue heating of the microcalorimeter by neutrons, our design deflects the x-ray flux from ITER with the aid of the grazing-

[a)]Contributed paper, published as part of the Proceedings of the 18th Topical Conference on High-Temperature Plasma Diagnostics, Wildwood, NJ, USA, May 2010.

 © 2010 American Institute of Physics

Downloaded 08 Mar 2011 to 128.183.169.235. Redistribution subject to AIP license or copyright; see http://rsi.aip.org/about/rights_and_permissions

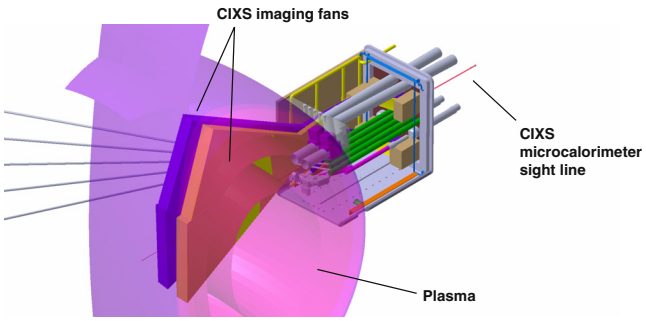

FIG. 1. (Color online) Conceptual design of the CIXS located in ITER's equatorial port plug showing the imaging fans of the crystal spectrometer elements and the line of sight for the x-ray microcalorimeter.

incidence mirror, as illustrated in Fig. 2. The mirror deflects the incoming x rays by about 0.5°. This amount of deflection is close to the upper limit for deflecting the 9.1 keV neonlike tungsten x-rays without debilitating losses.[3] This deflection means that over a 20 m distance, the incoming neutron beam defined by the initial 2–4 m long collimating aperture before bending by the grazing-incidence mirror will be separated from the x-ray beam by about 17 cm. This separation is sufficient to keep unscattered neutrons from hitting the microcalorimeter.

III. MICROCALORIMETER PERFORMANCE

Microcalorimeters have been primarily designed for rocket and space flight operation.[4–6] We have tested and operated several generations of microcalorimeters[7,8] at the Fusion and Astrophysics (FAST) Atomic Data and Diagnostic Calibration User Facility[9] at Livermore. An overview of the key performance parameters of microcalorimeters in the 2–12 keV range is given in Table I. We note that calorimeters also exist that specialize in hard x-ray (12–100 keV) measurements[10,11] and in soft x-ray measurements (<2 keV).

As Table I shows, progress in microcalorimeter performance has been rapid, and we can expect that the ITER instrument will have 1000–2000 pixels. Assuming a 40 ×40 pixel array, the total detector area will roughly be 144 mm^2. The photon count rate frequency the instrument will be able to handle without degradation of its 2.5 eV energy resolution will be 80 kHz. The instrument can handle count rates many times 80 kHz but only about 80 kHz can be analyzed with the highest resolution. The balance of the counts will yield somewhat lower spectral resolution.

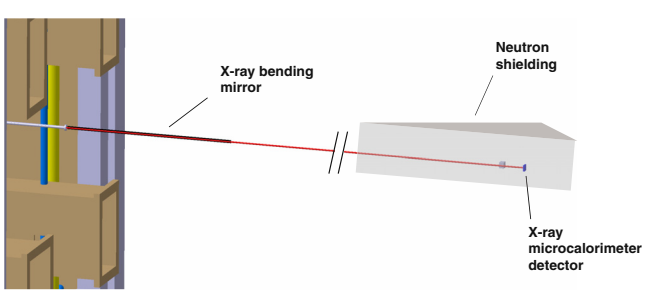

FIG. 2. (Color online) Details of the x-ray microcalorimeter line of sight. The detector is removed from the port plug by about 20 m.

TABLE I. Characteristics of past and future x-ray microcalorimeters employed at the electron beam ion trap based Livermore Fusion and Astrophysics (FAST) Atomic Data and Diagnostic Calibration User Facility.

Date of operation	Number of pixels	Energy resolution at 6 keV (eV)	Count rate (counts/s)
1996	1	25	≤1
2000	32	11	130
2003	32	5.5	130
2007	32	4.5	130
2011[a]	256	2.5	13 000
2015	>1000	2.5[b]	>50 000
ITER[c]	1600	2.5[b]	>80 000

[a]Expected year of installation on the FAST Facility.
[b]The intrinsic detector resolution is 1.8 eV; the quoted resolution includes maximum allocations for all system noise sources.
[c]Assuming a duplication of the device built for the International X-Ray Observatory (Ref. 12).

The event-mode output of a microcalorimeter is similar to other solid-state x-ray detectors, such as those used in pulse-height-analysis systems commonly employed on tokamaks, except with much better resolution. We illustrate this in Fig. 3, where we show a comparison of the x-ray emission recorded with a high-purity intrinsic germanium detector and the emission recorded concurrently with a microcalorimeter. An expanded view of the microcalorimeter spectrum from a different discharge at the Livermore calibration facility is shown in Fig. 4 to illustrate the performance for plasma impurity monitoring, while Fig. 5 shows the emission of highly charged tungsten over the full range of microcalorimeter sensitivity relevant for the CIXS diagnostic on ITER.

IV. POTENTIAL ION TEMPERATURE PROFILE MEASUREMENTS WITH THE MICROCALORIMETER

The 2.5 eV resolution of the CIXS microcalorimeter is sufficient to determine the core ion temperature from the Doppler broadening of the W^{64+} resonance line at 9.1 keV.

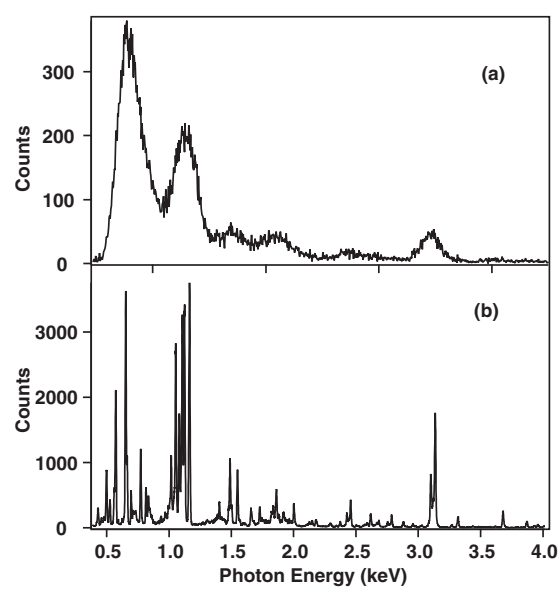

FIG. 3. Comparison of the x-ray emission observed concurrently with (a) a high-purity germanium detector and (b) a x-ray microcalorimeter.

Downloaded 08 Mar 2011 to 128.183.169.235. Redistribution subject to AIP license or copyright; see http://rsi.aip.org/about/rights_and_permissions

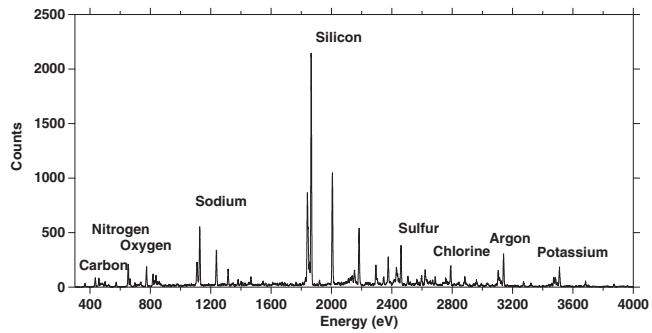

FIG. 4. Spectral emission recorded with an x-ray microcalorimeter on the Livermore Fusion and Astrophysics (FAST) Atomic Data and Diagnostic Calibration User Facility. The spectrum shows *K*-shell emission from various "impurity" ions, including carbon, nitrogen, oxygen, sodium, silicon, sulfur, and argon. Many of the elements were deliberately introduced for this illustration.

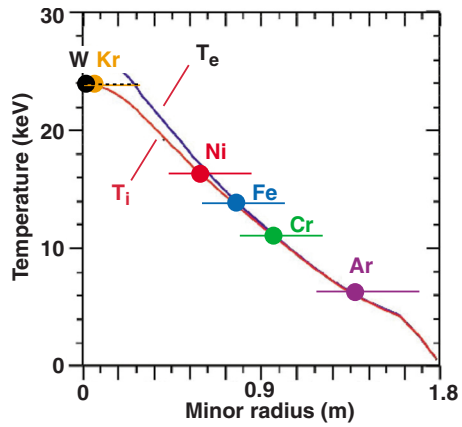

FIG. 6. (Color online) Expected ion temperature profile measurement based on line profile measurements of potential trace element ions using the CIXS microcalorimeter.

At an ion temperature of 24 keV, the width of this line will be 8 eV, which is well within the capabilities of the microcalorimeter instrument. Similarly, the line width of the Lyman-α line of hydrogenlike Fe^{25+} at the temperature of maximum emissivity (roughly 13 keV) is also about 8 eV. Even the 3 eV linewidth of the Lyman-α lines of Ar^{17+} at 6 keV can be used to determine the ion temperature, although this is probably the limit of the instrument.

The electron temperature of maximum emissivity for each ion species stems from the convolution of the emission rate and the ion abundance. This temperature is very roughly two times the energy of the *K*-shell x-ray transition emitted. From the temperature of maximum emission and a measured electron temperature profile, we can determine the approximate location from which the radiation was emitted in a similar fashion as was used for ion temperature profiles measurements employing ultraviolet lines.[13] In turn, this means that we can, in principle, correlate the ion temperature inferred from the linewidth with the plasma minor radius so that a crude radial ion temperature profile can be constructed. This is illustrated in Fig. 6. Detailed modeling calculations will be needed to demonstrate how well such measurements can localize a particular line emission and to determine the integration times needed for obtaining a reliable line profile given a high bremsstrahlung background.

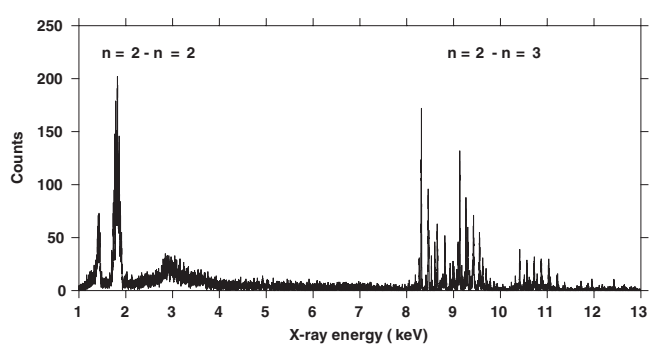

FIG. 5. Spectral emission of tungsten recorded with an x-ray microcalorimeter on the Livermore FAST Atomic Data And Diagnostic Calibration User Facility. The tungsten emission was produced at an electron beam energy of about 51 keV. For more information see Ref. 14.

V. OUTSTANDING DESIGN ISSUES

Several conceptual design issues still need to be addressed. These include the design of the absorber foils to achieve a flat response across the 2–10 keV x-ray band, while taking into account the intrinsic response of the x-ray mirror, and potential optimization of the count rate in certain key lines used for impurity concentration and possibly ion temperature measurements, in order to attain the quickest possible time response for the instrument. Moreover, the size and placement of the x-ray mirror are still under discussion.

A general issue affecting the workings of the entire CIXS system is the ability for any detector to withstand the neutron flux generated by ITER. A neutronics calculation will be performed when the port plug integration has been completed. The resulting predictions will be needed to assess the amount of scattered neutron flux at the location of a given detector and whether adequate shielding is possible.

ACKNOWLEDGMENTS

This work was performed under the auspices of the U.S. DOE by LLNL under Contract No. DE-AC52-07NA-27344 and supported in part by Memorandum Purchase Order ICP009477-R from the Princeton Plasma Physics Laboratory, the LLNL Laboratotry Directed Research and Development project 016-ERD-09, and NASA's Astronomy and Physics Research and Analysis program.

[1] P. Beiersdorfer, J. Clementson, J. Dunn, M. F. Gu, K. Morris, Y. Podpaly, E. Wang, M. Bitter, R. Feder, K. W. Hill, D. Johnson, and R. Barnsley, J. Phys. B **43**, 144008 (2010).
[2] C. K. Stahle, D. McCammon, and K. D. Irwin, Phys. Today **52**(8), 32 (1999).
[3] See the Lawrence Berkeley National Laboratory website at http://www-cxro.lbl.gov/ for mirror reflectivity.
[4] R. L. Kelley, M. D. Audley, K. R. Boyce, S. R. Breon, R. Fujimoto, K. C. Gendreau, S. S. Holt, Y. Ishisaki, D. McCammon, T. Mihara, K. Mitsuda, S. H. Moseley, D. B. Mott, F. S. Porter, C. K. Stahle, and A. E. Szymkowiak, Proc. SPIE **3765**, 114 (1999).
[5] D. McCammon, R. Almy, E. Apodaca, W. Bergmann Tiest, W. Cui, S. Deiker, M. Galeazzi, M. Juda, A. Lesser, T. Mihara, J. P. Morgenthaler, W. T. Sanders, J. Zhang, E. Figueroa-Feliciano, R. L. Kelley, S. H. Moseley, R. F. Mushotzky, F. S. Porter, C. K. Stahle, and A. E. Szymkowiak, Astrophys. J. **576**, 188 (2002).
[6] R. L. Kelley, K. Mitsuda, C. A. Allen, P. Arsenovic, M. D. Audley, T. G.

Downloaded 08 Mar 2011 to 128.183.169.235. Redistribution subject to AIP license or copyright; see http://rsi.aip.org/about/rights_and_permissions

Bialas, K. R. Boyce, R. F. Boyle, S. R. Breon, G. V. Brown, J. Cottam, M. J. Dipirro, R. Fujimoto, T. Furusho, K. C. Gendreau, G. G. Gochar, O. Gonzalez, M. Hirabayashi, S. S. Holt, H. Inoue, M. Ishida, Y. Ishisaki, C. S. Jones, R. Keski-Kuha, C. A. Kilbourne, D. McCammon, U. Morita, S. H. Moseley, B. Mott, K. Narasaki, Y. Ogawara, T. Ohashi, N. Ota, J. S. Panek, F. S. Porter, A. Serlemitsos, P. J. Shirron, G. A. Sneiderman, A. E. Szymkowiak, Y. Takei, J. L. Tveekrem, S. M. Volz, M. Yamamoto, and N. Y. Yamasaki, Publ. Astron. Soc. Jpn. **59**, 77 (2007).

[7] F. S. Porter, M. D. Audley, P. Beiersdorfer, K. R. Boyce, R. P. Brekosky, G. V. Brown, K. C. Gendreau, J. Gygax, S. Kahn, R. L. Kelley, C. K. Stahle, and A. E. Szymkowiak, Proc. SPIE **4140**, 407 (2000).

[8] F. S. Porter, P. Beiersdorfer, K. Boyce, G. V. Brown, H. Chen, J. Gygax, S. M. Kahn, R. Kelley, C. A. Kilbourne, E. Magee, and D. B. Thorn, Can. J. Phys. **86**, 231 (2008).

[9] G. V. Brown, P. Beiersdorfer, J. Dunn, E. Magee, J. Park, F. S. Porter, M. Schneider, E. Träbert, R. L. Kelley, and C. A. Kilbourne, Proc. SPIE **7732**, 77324Q (2010).

[10] D. B. Thorn, G. V. Brown, J. H. T. Clementson, H. Chen, M. H. Chen, P. Beiersdorfer, K. R. Boyce, C. A. Kilbourne, F. S. Porter, and R. L. Kelley, Can. J. Phys. **86**, 241 (2008).

[11] D. B. Thorn, M. F. Gu, G. V. Brown, P. Beiersdorfer, F. S. Porter, C. A. Kilbourne, and R. L. Kelley, Phys. Rev. Lett. **103**, 163001 (2009).

[12] R. L. Kelley, S. R. Bandler, W. B. Doriese, Y. Ezoe, R. Fujimoto, L. Gottardi, R. den Hartog, J. den Herder, H. Hoevers, K. Irwin, Y. Ishisaki, C. A. Kilbourne, P. de Korte, J. van der Kuur, K. Mitsuda, T. Ohashi, L. Piro, F. S. Porter, K. Sato, K. Shinozaki, P. Shirron, S. J. Smith, Y. Takei, P. Whitehouse, and N. Y. Yamasaki, in *American Institute of Physics Conference Series*, edited by B. Young, B. Cabrera, and A. Miller (AIP, New York, 2009), Vol. 1185, p. 757.

[13] S. Suckewer and E. Hinnov, Nucl. Fusion **17**, 945 (1977).

[14] J. T. Clementson, "Spectroscopic investigations of highly charged tungsten ions," Ph. D. thesis, Lund University, 2010.

Downloaded 08 Mar 2011 to 128.183.169.235. Redistribution subject to AIP license or copyright; see http://rsi.aip.org/about/rights_and_permissions